Molecular & Biochemical Parasitology xxx (xxxx) xxx–xxx

Contents lists available at ScienceDirect

Molecular & Biochemical Parasitology

journal homepage: www.elsevier.com/locate/molbiopara

Substrate specificity profiling of M32 metallocarboxypeptidases from *Trypanosoma cruzi* and *Trypanosoma brucei*

Alejandra P. Frasch[a,1], León A. Bouvier[a], Florencia M. Oppenheimer[a,2], Maria Aparecida Juliano[b], Luiz Juliano[b], Adriana K. Carmona[b], Juan José Cazzulo[a], Gabriela T. Niemirowicz[a,*]

[a] Instituto de Investigaciones Biotecnológicas Dr. Rodolfo A. Ugalde-Instituto Tecnológico de Chascomús (IIB-INTECH), Universidad Nacional de San Martín (UNSAM), Consejo Nacional de Investigaciones Científicas y Técnicas (CONICET), Campus Miguelete, Av. 25 de Mayo y Francia, 1650 San Martín, Buenos Aires, Argentina
[b] Departamento de Biofísica, Universidade Federal de São Paulo, São Paulo, Brazil

ARTICLE INFO

Keywords:
Metallocarboxypeptidases
FRET substrates
Trypanosoma cruzi
Trypanosoma brucei
Protease
Family M32

ABSTRACT

Metallocarboxypeptidases (MCPs) of the M32 family, while broadly distributed among prokaryotic organisms, have so far been only found in a few eukaryotes including trypanosomatids. Among these organisms are human and animal pathogens of medical relevance such as *Trypanosoma brucei* and *Trypanosoma cruzi*, the respective causative agents of sleeping sickness and Chagas disease. The M32 MCP orthologues found in these parasites share 72% protein sequence identity. They also present a cytosolic localization, a similar pattern of expression and a marked preference for Arg/Lys residues at P1′. To further explore MCPs substrate specificity beyond the S1′ subsite, we employed four positional scanning synthetic combinatorial libraries (PS-SC) of fluorescence resonance energy transfer (FRET) peptides. Our results indicated that the *T. brucei* enzyme has a restricted selectivity for Phe in P1 position compared to *T. cruzi* MCP-1, which presented a wider range of substrate acceptance. The S2, S3 and S4 subsites, on the other hand, could accommodate a broad range of residues. On the basis of these results, we synthesized for each enzyme a series of FRET substrates which contained the most favourable residues in every position. In particular, for both MCPs acting on FRET pentapeptide substrates, catalytic efficiencies were ~100 times higher compared with previously described chromogenic substrates. In fact, the fluorogenic peptide Abz-LLKFK(Dnp)-OH (Abz = *ortho*-aminobenzoic acid; Dnp = 2, 4-dinitrophenyl) described here can be used to monitor accurately *Tb*MCP-1 activity in parasite cell-free extracts. These results provide valuable insights to develop selective substrates and inhibitors, to further understand the mechanisms and functions of M32 MCPs.

1. Introduction

Carboxypeptidases (CPs) are a group of hydrolases that perform many diverse physiological functions by removing C- terminal amino acids from proteins and peptides. These enzymes are important mediators of cellular behavior that can alter protein functionality and participate in proteome turnover [1] including vast and diverse processes such as protein trafficking, subcellular anchoring and the formation of macromolecular complexes [2,3]. CPs also modulate different signaling pathways and are connected to various pathological processes like carcinogenesis as well as neurodegenerative and cardiovascular diseases [1]. According to the chemical nature of their catalytic site, these hydrolases can be divided into three major classes, namely serine carboxypeptidases, cysteine carboxypeptidases, and metallocarboxypeptidases (MCPs), with the latter group usually employing zinc as a catalytic cofactor. Among MCPs, the M32 or *Thermus aquaticus* carboxypeptidase (*Taq*CP) family consists of a large number of enzymes with broad specificity. This family, which possesses the classical HEXXH motif observed in numerous zinc metalloproteases, is broadly distributed among prokaryotic organisms, but so far it has been found only in a few eukaryotes, namely some green algae and trypanosomatids [4,5].

The Trypanosomatidae family comprises several species that cause highly disabling and often fatal diseases such as sleeping sickness,

Abbreviations: Abz, *ortho*-aminobenzoic acid; Dnp, 2, 4-dinitrophenyl; FRET, fluorescence resonance energy transfer; MCP, metallocarboxypeptidase; MOPS, 3-(N- morpholino)propanesulfonic acid; PS-SC, positional scanning synthetic combinatorial; *Tb*MCP-1, *Trypanosoma brucei* metallocarboxypeptidase-1; *Tc*MCP-1, *Trypanosoma cruzi* metallocarboxypeptidase-1

* Corresponding author.
E-mail address: gniemiro@iibintech.com.ar (G.T. Niemirowicz).
[1] Present address: Department of Microbiology, Tumor and Cell Biology (MTC), Karolinska Institutet, Box 280, Nobels väg 16, 171 77 Stockholm, Sweden.
[2] Present address: Fundación Pablo Cassara-ICT Milstein-CONICET.

https://doi.org/10.1016/j.molbiopara.2017.12.001
Received 12 September 2017; Received in revised form 4 December 2017; Accepted 11 December 2017

Chagas disease and Leishmaniasis. The current chemotherapy used in the treatment of these infections presents serious side effects, and in some cases has low effectiveness, which underscores the necessity to develop new chemotherapeutic compounds. In this scenario, proteases have become popular candidates for drug targets since they accomplish both housekeeping tasks common to many eukaryotes as well as functions highly specific to the parasite life style. For example, cruzipain, a cysteine protease belonging to the family C1, which is also an immunodominant antigen in human chronic Chagas disease [6], promotes mammalian cell invasion by *Trypanosoma cruzi* trypomastigotes and also plays a major role in the differentiation steps of the parasite's life cycle [7,8]. Although several cruzipain inhibitors efficiently kill the parasite [7,8], developing new drugs for this or other proteases has been a challenging task, due to issues such as the difficulty of achieving selectivity when targeting their active sites. In this context, the absence of M32 MCPs in metazoans constitutes an attractive trait considering the high specificity/selectivity potential of this family. In particular, *T. cruzi*, *T. brucei* and *Leishmania* spp. contain conserved M32 MCPs, which have been characterized [4,5,9–12]. Nonetheless, to date, no inhibitors or biological functions have been reported for these enzymes. On the basis of their biochemical properties and stage-specific expression, *L. major* M32 carboxypeptidase (*Lma*CP1) has been implicated in the catabolism of peptides and proteins to single amino acids required for protein synthesis [10]. Other possible functions have also emerged through the determination of the crystal structure of *T. cruzi* metallocarboxypeptidase 1 (*Tc*MCP-1) [11]. This enzyme shows a strong structural resemblance to archaeal, bacterial and mammalian metallopeptidases including angiotensin I- converting enzyme, neurolysin and thimet oligopeptidase [11]. These evidences, plus the restricted substrate preference of *Tc*MCP-1 [4], have also pointed out to a possible regulatory role in the metabolism of small peptides. In fact, it has been shown that *Tc*MCP-1 can produce des-Arg9 bradykinin by hydrolysis of bradykinin [9]. This peptide is known to promote the process of mammalian cell invasion by the *T. cruzi* trypomastigotes through B1 receptors [13]. Recently, two reports have suggested that M32 peptidases are secreted by trypanosomatids [14,15] , a fact that might make feasible the latter hypothesis.

In this work we extended the substrate specificity (P1 to P4 position) analysis of *Tc*MCP-1 and *Tb*MCP-1, two trypanosomatid M32 MCPs that remove basic C-terminal residues, using positional scanning synthetic combinatorial (PS-SC) libraries of fluorescence resonance energy transfer (FRET) peptides. These results might contribute to generate new tools to identify the roles these proteases play in the parasite biology as well as to aid in the development of selective assays and specific inhibitors.

2. Materials and methods

2.1. Enzymes

*Tc*MCP-1, *Tb*MCP-1 and *Tb*MCP-1 A414M were expressed as GST fusion proteins in *E. coli* BL21 (DE3) Codon Plus and purified as previously described [9,11].

2.2. Synthesis of peptide libraries

PS-SC libraries were synthesized by the methods previously described [16,17] except that the Abz (*ortho*-aminobenzoic acid) and Dnp (2, 4-dinitrophenyl) groups were used as the fluorescence donor and acceptor pairs, respectively. For preliminary experiments, we employed a library with the general structure Abz-GXXZXK(Dnp)-OH, where the Z position was successively replaced with one of the 19 amino acids (Cys excluded) and X represents a randomly incorporated residue introduced by coupling a balanced mixture of 19 amino acids [18]. The other three libraries presented the structures Abz-GXXRZK(Dnp)-OH, Abz-GXZRXK (Dnp)-OH, and Abz-GZXRXK(Dnp)-OH, in which two of the positions were fixed: the P2 position as Arg and Z as P1, P3, and P4 which included 19 naturally occurring amino acids with the other positions randomized (Cys excluded). For synthesis details see reference [18]. Stock solutions of each peptide mixture were prepared in DMSO, and the concentrations were measured using the absorbance of Dnp, with a molar extinction coefficient ε_{365nm} of 17 300 $M^{-1}\,cm^{-1}$.

2.3. Screening of peptide libraries

Peptide libraries were screened at 25 nM final concentration to ensure the hydrolysis of the K(Dnp)-OH group to be directly proportional to the specificity constant, k_{cat}/K_M. Reactions were initiated by the addition of the enzyme (50–100 nM) and monitored in a Hitachi F-2000 fluorescence spectrophotometer (Hitachi High-Technologies Corporation, Tokyo, Japan) by measuring the fluorescence at 420 nm (λ_{em}) and 320 nm (λ_{ex}). Assays were done at 25 °C in 0.1 M MOPS (3-(N-morpholino)propanesulfonic acid) buffer pH 7.3. For k_{cat}/K_M estimation, only data in the linear portion of the progression curve was considered (first order condition: $[S] << K_M$) [16].

Optimal substrates (purity > 95%) for both MCPs were synthesized by GenScript (Piscataway, NJ, USA). Assays were performed at 25 °C, in 0.1 M MOPS pH 7.3. Enzymatic activity was continuously followed in an AMINCO®-Bowman Series 2 spectrofluorometer (Thermo Spectronic, Madison, WI, USA) by measuring the fluorescence at 420 nm (λ_{em}) and 320 nm (λ_{ex}). The enzyme concentration for the initial rate determination was chosen so that less than 5% of the substrate present was hydrolyzed. The slope was converted into micromoles of substrate hydrolyzed per minute based on a calibration curve obtained from complete hydrolysis of each peptide. The kinetic parameters K_M and k_{cat} were calculated using GraphPad Prism software (GraphPad Software Inc, La Jolla, CA, USA).

2.4. Trypanosome culture

Bloodstream form *T. brucei brucei* cell line 90:13 (tetR-HYG T7RNAPOL-NEO) [19] was cultured at 37 °C under 5% CO_2 in HMI-9 medium (Sigma- Aldrich, St. Louis, MO, USA) [20] supplemented with 10% fetal bovine serum plus 2.5 μg/mL of G418 (Thermo Fisher Scientific, Waltham, MA, USA) and 5 μg/mL of hygromycin B (InvivoGen, San Diego, CA, USA).

2.5. Generation of TbMCP-1 null mutant cell lines

For a detailed description of *TbMCP-1* gene replacement cassettes, see Supplementary Material. For each transfection, approximately 2×10^7 trypanosomes grown to mid log phase ($\sim 0.8–1.0 \times 10^6$ cells/mL) in HMI-9 medium, were collected, washed once in citomix (2 mM EGTA, 120 mM KCl, 0.15 mM $CaCl_2$, 10 mM K_2HPO_4/KH_2PO_4 pH 7.6, 25 mM HEPES pH 7.6, 5 mM $MgCl_2{\cdot}6H_2O$, 0.5% glucose, 100 μg/mL BSA, 1 mM hypoxanthine) at room temperature and resuspended in 500 μL of the same buffer. About 5–15 μg of linearized plasmid was mixed into the cell suspension and transferred to a BTX 0.2 cm electroporation cuvette. Electroporation was immediately performed at a single pulse with a BTX 600 Electro Cell Manipulator (BTX Inc., San Diego, CA, USA) at 1.1 kV, 25 μF and R6 resistance (186 Ω). The entire cell-DNA mixture was transferred to a flask containing 5 mL of fresh HMI-9 medium and incubated 6 h at 37 °C without selection. Cells were diluted to a density of 2×10^5 cell/mL and 1 mL cell aliquots were distributed in 24-well plates. Selection was achieved by the addition of 2.5 μg/mL G418, 5 μg/mL hygromycin B plus 10 μg/mL of blasticidin S (InvivoGen) and/or 0.1 μg/mL of puromycin (InvivoGen).

2.6. Preparation of parasite extracts

T. brucei bloodstream trypomastigotes were broken by three cycles of freezing at −20 °C and thawing. The parasite pellets were extracted

with 0.1 M MOPS pH 7.3, containing 1 mM PMSF and 10 μM E-64 [trans-epoxysuccinyl-L-leucylamido-(4- guanidino)butane]. The preparation was centrifuged at 26900*g* for 30 min at 4 °C. The pellet was extracted again with the same buffer and centrifuged under identical conditions. The combined supernatants were centrifuged at 26900*g* for 30 min at 4 °C. The cell-free extract was retained and the pellet was discarded. Activity on the substrate Abz-LLKFK(Dnp)-OH (10 μM) was assayed in 0.1 M MOPS pH 7.3 as described before.

2.7. Electrophoresis and immunoblotting

Approximately $1{,}5 \times 10^7$ parasites from *Tb*MCP-1 mutant cell lines were resuspended in 1X Laemmli sample buffer, heated in boiling water for 5 min and separated by SDS-PAGE (10% acrylamide). Gels were transferred to a nitrocellulose Hybond ECL membrane (GE Healthcare, Pittsburgh, PA, USA) for probing with anti *Tb*MCP-1 mouse polyclonal antibody diluted 1:200 [9]. Polyclonal rabbit anti enolase 1:1000 [21] was used as loading control. Blots were probed with Alexa Fluor® 790 AffiniPure Goat Anti-Mouse IgG (H + L) or Alexa Fluor® 680 AffiniPure Goat Anti-Rabbit IgG (H + L) secondary antibodies (Jackson Immunoresearch Laboratories, West Grove, PA, USA). Signal intensities were detected using an Odyssey laser-scanning system and quantified with Image Studio software (LI-COR Biosciences, Lincoln, NE, USA). Prestained Protein Molecular Weight markers used were from Pierce (Rockford, IL, USA).

3. Results

3.1. FRET libraries

Most of the work already done on M32 MCPs has been focused on analysing the substrate specificity of these enzymes for the P1′ position, not taking into account the contribution of the non-prime sites. In order to explore the S1 to S4 substrate preference of M32 peptidases an already available combinatorial peptide library designed for somatic angiotensin I- converting enzyme (ACE)[22] was used. As ACE is a carboxydipeptidase, to study the P1 preference of this enzyme this library was originally synthetized with the general structure Abz-GXXZXK(Dnp)-OH were Z corresponds to each amino acid residue to be evaluated. Since M32 enzymes are carboxymonopeptidases, we first investigated if these peptides could be used by this protein family. Due to the fixed Lys(Dnp)-OH at the C-terminus of the peptide library, we employed two M32 MCPs, *Tc*MCP-1 and *Tb*MCP-1, which have similar basic amino acid preference at P1′ position and share 71% of protein sequence identity [4,9].

Specificity constants (k_{cat}/K_M) for the hydrolysis of Abz-GXXZXK (Dnp)-OH peptide series are shown in Fig. 1P2. *Tc*MCP-1 activity is favoured by the presence of basic (Lys, Arg) or aromatic (Phe, Tyr) amino acids at P2 position. Peptides containing other hydrophobic residues, especially aliphatic (Val, Leu, Ile) were also cleaved by the *T. cruzi* enzyme. For *Tb*MCP-1 maximal activity was achieved with Lys at P2 position. In general both orthologs followed the same hydrolysis pattern. Notably the occupancy of the S2 subsite by negative charged amino acids (Asp and Glu) resulted in almost no peptide hydrolysis by both trypanosomatid MCPs.

On the light of these results we decided to extend this study to the analysis of *Tc*MCP-1 and *Tb*MCP-1 S1, S3 and S4 subsite preference. For this purpose we used three other sublibraries previously designed for ACE: Abz-GXXRZK(Dnp)-OH, Abz-GXZRXK(Dnp)-OH, and Abz-GZXRXK(Dnp)-OH (Fig. 1). In particular, the P1 position resulted to be the most informative. Both MCPs strongly preferred Phe in this position. Notably the *T. brucei* enzyme presented a significant selectivity for this residue at S1, those peptides containing Phe been hydrolysed with the highest k_{cat}/K_M values (Fig. 1P1). *Tc*MCP-1, on the other hand, can equally employ Arg or Thr at P1. Among non-polar amino acids, the *T. cruzi* enzyme could not cleave those branched at beta carbon (Val, Ile). Again, negatively charged amino acids residues have a deleterious effect on the specificity constants of both enzymes.

Analysis of P3 and P4 positions was less informative (Fig. 1P3 and 1P4). In particular positively charged amino acid residues were preferred by the S3 subsite of both enzymes. Sequences containing non-polar aliphatic residues at P3 were also hydrolysed by *T. cruzi* MCP with similar k_{cat}/K_M values (Fig. 1P3). *Tb*MCP-1, on the other hand, tended to favour Leu and Met at this position, the former being the best substrate of this series.

MCPs S4 subsite can accommodate bulky aromatic and positively charged residues with similar specificity constants (although one exception is His for *Tb*MCP-1). The use of residues such as Asn, Gln and Ser, to a lower extent, takes relevance at S4. Similar specificity constants were registered at this position, thus showing the lack of selectivity of this subsite. Nonetheless, differences between both enzymes could be found, in particular the capacity of *Tc*MCP-1 of handling aliphatic residues with higher specificity constants. Again substrates containing Glu and Asp at P3 or P4 positions were resistant to hydrolysis by both MCPs or had low k_{cat}/K_M values. A similar observation was made for small amino acids such as Gly and Pro, which present low k_{cat}/K_M values across this series.

3.2. Testing the S1 subsite

Previously we had described a P1 specificity mutant of *Tb*MCP-1 for which the sole replacement of residue Ala 414 by Met (amino acid residue found at the same position in *Tc*MCP-1) resulted in gain of activity against a tripeptide substrate [9]. In order to explore if this substitution could in part explain the broad S1 specificity of *Tc*MCP-1, we measured *Tb*MCP-1 A414M activity against the P1 sublibrary. As shown in Fig. 2 this mutant tended to gain little activity against peptides containing positively (Lys, Arg, His) and negatively (Asp, Glu) charged amino acids residues at P1 position. Branched chain residues, namely Ile and Val, were also hydrolysed with a ~3.7 and 9 fold relative activity increase, respectively. Other amino acid residues including Asn and Ser were better hydrolysed by mutant A414M than by the wild-type *Tb*MCP-1.

3.3. MCPs activity on FRET substrates derived from peptide libraries

Based on the library results shown in Fig. 1, best tri-, tetra- and pentapeptide FRET substrates were synthetized for each MCP. Their kinetic parameters and V vs. [S] plots are summarized in Table 1 and Fig. S2, respectively. For *Tc*MCP-1 there was a direct correlation between k_{cat}/K_M values and the length of the substrate for both peptide series analysed (Fig. S3). With the exception of Abz-RRFFK(Dnp)-OH, for the *T. brucei* enzyme the substrate affinity dropped conforming peptide length increased although higher V_{max} values were obtained with both pentapeptides.

3.4. M32 MCP null mutant strains

To gain insights into the functions of M32 MCPs in trypanosome physiology as well as to determine the essentiality of these enzymes we sought to obtain null mutant parasite strains. Initially, attempts to disrupt both *TcMCP-1* genes by sequential transfection of selectable marker based disruption constructs into insect stage epimastigotes from *T. cruzi* turned out to be unsuccessful. While the first allele could readily be deleted, the second *TcMCP-1* gene remained refractory to replacement by the disruption construct, which in addition, was kept as an episome (data not shown). Although the several failed attempts suggested an essential role for *Tc*MCP-1 it was likely that these were due, to some extent, to the known difficulties associated with gene replacement methodologies in *T. cruzi* [23]. Consequently we considered to conduct a similar undertaking with *T. brucei* 90:13 strain, which is more amenable to genetic manipulation, and to focus on the bloodstream

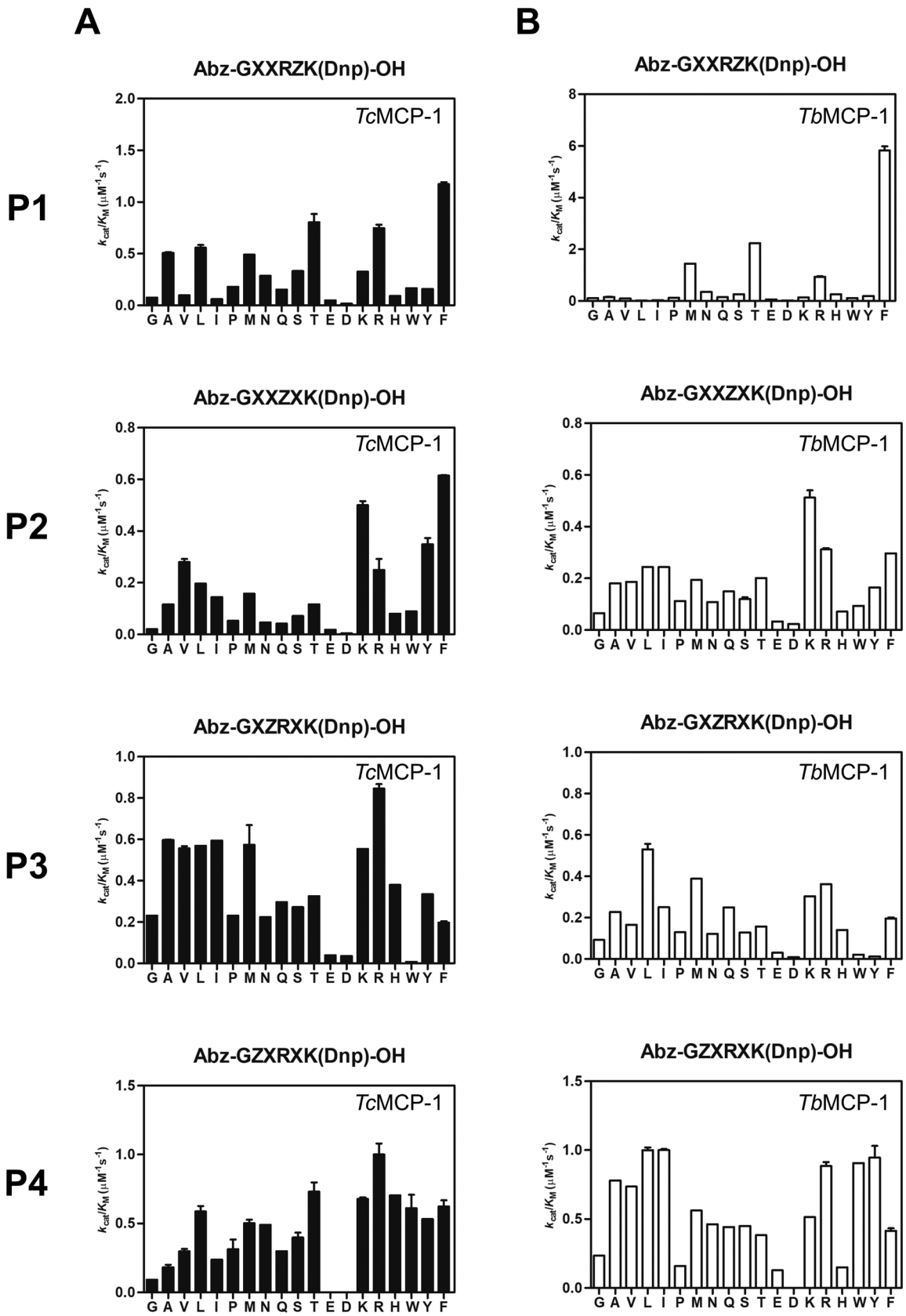

Fig. 1. Combinatorial fluorescence-quenched peptide libraries for scanning of subsites P4-P1. The libraries with Abz-GXXZXK(Dnp)-OH (P2), Abz-GXZRXK(Dnp)-OH (P3), Abz-GZXRXK (Dnp)-OH (P4), and Abz-GXXRZK (Dnp)-OH (P1) general sequences were incubated with recombinant *Tc*MCP-1 (panel A) and *Tb*MCP-1 (panel B) as described in Materials and Methods section. The assays were performed at low substrate concentrations where the reactions followed first-order conditions. The x axis shows the amino acids in the position that was investigated. The data represent the means ± S.D. of two replicates.

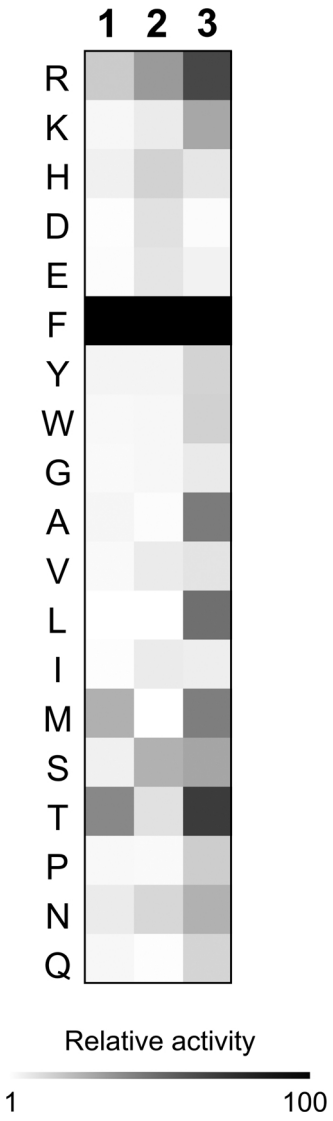

Fig. 2. Analysis of *Tb*MCP-1 A414 M P1 substrate specificity. The S1 subsite specificity of recombinant *Tb*MCP-1 (1) and *Tb*MCP-1 A414 M (2) was compared to that of *Tc*MCP-1(3). The heat map was normalized relative to the best substrate for each peptidase.

trypomastigote stage associated to the vertebrate host. According to Western blot analysis, deletion of the first allele conduced to a 2-fold reduction in *Tb*MCP-1 protein expression (Fig. 3A, HKO) which manifested as a delay from 6.46 to 6.8 h in the doubling time (Fig. 3B, HKO). Disappearance of the band relative to *Tb*MCP-1 from the Western blot confirmed the disruption of the second allele (Fig. 3A, KO). Although these results indicate that *Tb*MCP-1 is not essential for *T. brucei* growth under *in vitro* culture conditions, loss of this activity represented a further extension of the doubling time to 7.18 h (Fig. 3B, KO). Statistical analysis revealed that the reduced fitness of both HKO and KO parasite lines, in terms of longer doubling times, was significant ($P^{**} = 0.0049$, ANOVA).

3.5. Monitoring *Tb*MCP-1 activity in cell-free extracts

To determine the feasibility of specifically detecting M32 MCP activity in complex samples we conducted FRET peptide hydrolysis assays on cell free extracts. As substrate the peptide Abz-LLKFK(Dnp)-OH on which *Tb*MCP-1 showed the highest catalytic efficiency was chosen. In samples relative to wild-type *T. brucei* bloodstream trypomastigotes, peptide hydrolysis was 1.4 RFU/mg. The decrease in the specific activity detected in the extracts obtained from single null mutant parasites (HKO) evidenced that the activity was mainly due to *Tb*MCP-1. Furthermore, according to the assays performed on null mutant strain (KO) samples, native *Tb*MCP-1 accounted for ~83% of the detectable activity in wild-type cells (Fig. 4).

4. Discussion

Many studies have focused on the P1′ substrate specificity profile of M32 MCPs [10,24–26] whereas the contribution of the nonprime sites or possible cooperative effects of the substrate binding, has not been explored. The use of PS-SC FRET libraries allowed us to perform a fast and exhaustive survey of a large number of residue-subsite combinations that revealed notorious differences between trypanosomatid M32 MCPs. In this sense, *Tb*MCP-1 almost exclusively hydrolysed at the carbonyl group of Phe at P1 position. To a lower extent, Thr and Met, were also cleaved by the *T. brucei* enzyme but with ~2.6 and 4 decrease in the catalytic efficiency, respectively. On the other hand, *Tc*MCP-1, although being highly selective for Phe at P1 (k_{cat}/K_M ratio ~27), could hydrolyse a broader substrate repertoire. Interestingly, several amino acid differences within the proposed S1 pocket of the enzyme of *T. cruzi* [11] were found in *Tb*MCP-1, including the A408 V and A414 M substitutions. In this sense, we showed that the replacement of alanine 414 by a methionine residue, although not entirely mimicking the *Tc*MCP-1 P1 specificity profile, increased *Tb*MCP-1 promiscuity. Other substitutions, namely I408 V or F411S, did not improve *T. brucei* enzyme specificity against the P1 library (data not shown). In a fashion analogous to that proposed for other proteases [27], we cannot rule out the possibility that other regions, besides the S1 pocket, could be influencing the binding of the substrate. Moreover, recent studies suggest that M32 MCPs experiment a transition between an open and closed conformation upon substrate binding [28,29] which eventually could have implications in substrate recognition and catalysis.

For *Tc*MCP-1, the use of peptide substrates derived from the library screening revealed an increase in the k_{cat}/K_M values which is directly correlated with the chain length of the FRET peptide analysed (Fig. S3A). The increase in the catalytic efficiency is mainly due to a steady decrease in the K_M value, suggesting that interactions with the backbone atoms of the substrate also contribute to an efficient catalysis. The

Table 1
Kinetic parameters for the hydrolysis of FRET peptides by recombinant *Tc*MCP-1 and *Tb*MCP-1[a].

	*Tc*MCP-1			*Tb*MCP-1		
Peptide	K_M (μM)	k_{cat} (s^{-1})	k_{cat}/K_M (s^{-1} μM^{-1})	K_M (μM)	k_{cat} (s^{-1})	k_{cat}/K_M (s^{-1} μM^{-1})
Abz-FFK(Dnp)-OH	1.71 ± 0.18	0.85 ± 0.03	0.50	1.16 ± 0.10	11.79 ± 2.11	10.14
Abz-RFFK(Dnp)-OH	1.08 ± 0.29	2.39 ± 0.20	2.21	2.51 ± 0.50	1.57 ± 0.13	0.63
Abz-RRFFK(Dnp)-OH	0.37 ± 0.03	2.33 ± 0.05	6.30	0.37 ± 0.06	4.13 ± 0.19	11.60
Abz-KFK(Dnp)-OH	1.23 ± 0.20	1.25 ± 0.06	1.02	0.91 ± 0.12	6.92 ± 0.26	7.60
Abz-LKFK(Dnp)-OH	0.57 ± 0.09	1.17 ± 0.04	2.05	2.27 ± 0.63	6.04 ± 0.59	2.65
Abz-LLKFK(Dnp)-OH	0.54 ± 0.10	1.58 ± 0.08	2.92	2.43 ± 0.39	36.88 ± 2.27	15.12

[a] The assays were performed at 25 °C in 0.1 M MOPS pH 7.3. Measurements were made as described in Materials and Methods. The K_M errors represent standard error on the fit.

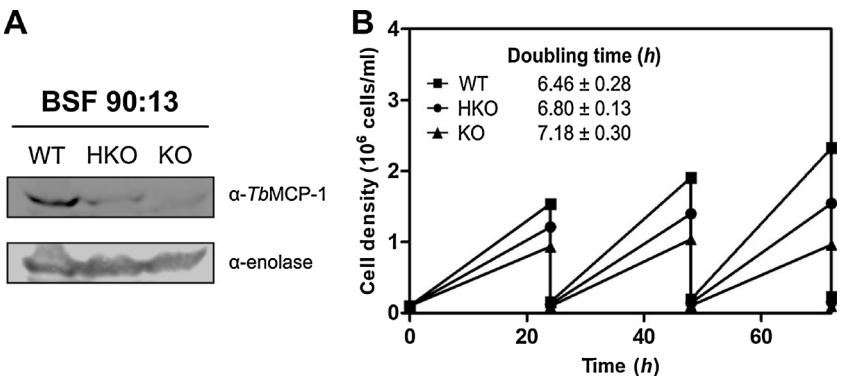

Fig. 3. Analysis of *Tb*MCP-1 mutant cell lines. (A) Approximately $1{,}5 \times 10^7$ parasites from wild-type (WT) 90:13 bloodstream trypomastigotes, and derived single (HKO) and double (KO) null mutant *Tb*MCP-1 cell lines, were analysed by Western blot using anti-*Tb*MCP-1 polyclonal antibodies [9]. Rabbit anti-enolase is shown as loading control [21]. Note that the band corresponding to *Tb*MCP-1 (~ 55 kDa) is absent in KO cells. (B) Growth curves of the WT, HKO and KO cell lines. Bloodstream cultures were initiated at 1×10^5 cells/mL and daily diluted 1/10. Doubling times (mean ± S.D. from 3 to 5 experiments) are indicated on the left of the figure ($P^{**} = 0.0049$, ANOVA).

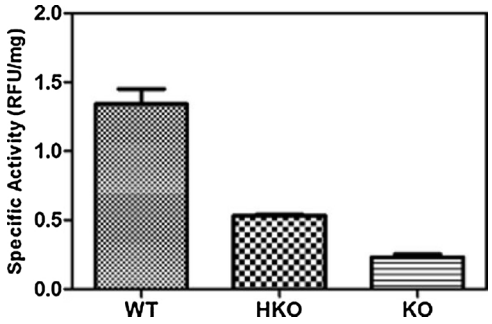

Fig. 4. Monitoring *Tb*MCP-1 activity in cell free-extracts. Cell-free extracts were prepared from wild-type (WT) bloodstream trypomastigotes, single (HKO) and null mutants (KO) *TbMCP-1* strains. The substrate Abz-LLKFK(Dnp)-OH was used at 10 µM final concentration in buffer 0.1 M MOPS pH 7.3 as described in the Materials and Methods section. The data represent the means ± S.D. of two independent experiments. ($P^{***} = 0.0005$, ANOVA).

best substrate, the pentapeptide Abz-RRFFK(Dnp)-OH, was ~13 fold more reactive than the corresponding tripeptide analysed (Table 1). These results point out the importance of having an extended substrate conformation able to interact with the *Tc*MCP-1 substrate-binding groove. Best catalytic efficiencies were also achieved with pentapeptide substrates for *Tb*MCP-1. Interestingly, for this enzyme, the increase in the length of the substrate did not lead to a decrease in the K_M values, but instead resulted in higher turnover numbers for the KFK series. These results indicate that for the *T. brucei* enzyme, the S1 and S1′subsites might be playing the most prominent role in substrate binding. In fact, there is little difference between the kinetic parameters obtained for the Abz-FFK(Dnp)-OH and Abz-KFK(Dnp)-OH substrates, both peptides sharing identical P1 and P1′ residues (Table 1). The P4 position, on the other hand, although not having high selectivity, contributed to a great extent to an efficient peptide hydrolysis. In this sense, the particular kinetic behaviour of both MCPs could reflect their functions and/or the concentration of a putative substrate *in vivo*. Thus, for example, for *Tc*MCP-1, having a low K_M might be more important than a high k_{cat} value when acting on peptide hormones, such as bradykinin [9]. Alternatively, the turnover number may be the critical parameter in situations where substrate concentration is high and a rapid substrate turnover is required, such as the case of *Tb*MCP-1 working together with proteasomes, ATP-dependent proteases, and other peptidases that could facilitate parasite growth through the rapid catabolism of peptides and proteins to the single amino acids, as proposed for the leishmanial enzyme [10].

Several colorimetric assays using synthetic substrates have been described to monitor the activity of M32 MCPs [4,24]. However, some techniques commonly used with this family, namely the ninhydrin method, have limitations, such as a laborious procedure and low sensitivity. The catalytic efficiencies of *Tc*MCP-1 and *Tb*MCP-1 acting on Abz-RRFFK(Dnp)-OH and Abz-LLKFK(Dnp)-OH substrates were ~91-fold and 123-fold higher, respectively, compared with the best colorimetric substrate FA-Ala-Lys [9]. This advantage allowed the detection of *Tb*MCP-1 mediated hydrolysis of the latter FRET substrate in complex cell free extracts. Comparative assays between samples derived from wild-type and null mutant bloodstream trypomastigotes indicated that this protease accounts for ~83% of the activity. Further peptide substrate optimization will be required to diminish the remaining residual activity, which is likely the result of unspecific cleavage by other endo- or exo-peptidases present in the sample. Nevertheless, the FRET substrates designed herein constitute good starting points for the development of derivatives with improved specificity and the strains obtained are valuable tools in accomplishing this task. In this sense, the success in obtaining the *Tb*MCP-1 null mutant *T. brucei* bloodstream trypomastigote cell line hints at a non-essential role of these proteases for parasite growth under *in vitro* culture conditions. Nevertheless, parasite doubling time increased significantly with each successive loss of *TbMCP-1* gene. This delay represents a twofold reduction in null mutant parasite density for every 72 h culture passage cycle, highlighting the contribution of these enzymes to parasite adaptive fitness. Further work will have to be conducted to evaluate the essentiality of M32 MCP activity in a trypanosome infection model.

Conflict of interest

The authors declare no conflict of interest.

Acknowledgements

This study was supported by PICT 2014-3510 from the Agencia Nacional de Promoción Científica y Tecnológica (ANPCyT, MinCyT), PIP CONICET 112-201301-00303 and the Bunge y Born Foundation to GTN. LAB, JJC and GTN are members of the research career of the Argentinean National Research Council (CONICET). The present work was done in the framework of the Red CYTED-PROMAL 210RT0398 (Proteómica y Quimiogenómica de Inhibidores de Proteasas de Origen Natural con Potencial Terapéutico en Malaria).

Appendix A. Supplementary data

Supplementary data associated with this article can be found, in the online version, at https://doi.org/10.1016/j.molbiopara.2017.12.001.

References

[1] A. Petrera, Z.W. Lai, O. Schilling, Carboxyterminal protein processing in health and disease: key actors and emerging technologies, J. Proteome Res. 13 (2014) 4497–4504.
[2] S. Tanco, K. Gevaert, P. Van Damme, C-terminomics: targeted analysis of natural and posttranslationally modified protein and peptide C-termini, Proteomics 15 (2015) 903–914.
[3] J.J. Chung, S. Shikano, Y. Hanyu, M. Li, Functional diversity of protein C- termini: more than zipcoding, Trends Cell Biol. 12 (2002) 146–150.

[4] G. Niemirowicz, F. Parussini, F. Aguero, J.J. Cazzulo, Two metallocarboxypeptidases from the protozoan *Trypanosoma cruzi* belong to the M32 family, found so far only in prokaryotes, Biochem. J 401 (2007) 399–410.
[5] G.T. Niemirowicz, A.P. Frasch, J. José Cazzulo, Chapter 280- Carboxypeptidase Taq-Like Peptidases from Trypanosomatids, in: N. Rawlings, G. Salvesen (Eds.), Handbook of Proteolytic Enzymes, Academic Press, Massachusetts, 2013, pp. 1253–1257.
[6] J. Martinez, O. Campetella, A.C. Frasch, J.J. Cazzulo, The major cysteine proteinase (cruzipain) from *Trypanosoma cruzi* is antigenic in human infections, Infect. Immun. 59 (1991) 4275–4277.
[7] V.E. Alvarez, G.T. Niemirowicz, J.J. Cazzulo, The peptidases of *Trypanosoma cruzi*: digestive enzymes, virulence factors, and mediators of autophagy and programmed cell death, Biochim. Biophys. Acta 1824 (2012) 195–206.
[8] J.J. Cazzulo, Chapter 438- Cruzipain, in: N. Rawlings, G. Salvesen (Eds.), Handbook of Proteolytic Enzymes, Academic Press, Massachusetts, 2013, pp. 1913–1918.
[9] A.P. Frasch, A.K. Carmona, L. Juliano, J.J. Cazzulo, G.T. Niemirowicz, Characterization of the M32 metallocarboxypeptidase of *Trypanosoma brucei*: differences and similarities with its orthologue in *Trypanosoma cruzi*, Mol. Biochem. Parasitol. 184 (2012) 63–70.
[10] C.E. Isaza, X. Zhong, L.E. Rosas, J.D. White, R.P. Chen, G.F. Liang, et al., A proposed role for *Leishmania major* carboxypeptidase in peptide catabolism, Biochem. Biophys. Res. Commun. 373 (2008) 25–29.
[11] G. Niemirowicz, D. Fernandez, M. Sola, J.J. Cazzulo, F.X. Aviles, F.X. Gomis- Ruth, The molecular analysis of *Trypanosoma cruzi* metallocarboxypeptidase 1 provides insight into fold and substrate specificity, Mol. Microbiol. 70 (2008) 853–866.
[12] C.E. Isaza, Chapter 279- Carboxypeptidase *Taq*, in: N. Rawlings, G. Salvesen (Eds.), Handbook of Proteolytic Enzymes, Academic Press, Massachusetts, 2013, pp. 1249–1253.
[13] A.G. Todorov, D. Andrade, J.B. Pesquero, R. de C. Araujo, M. Bader, J. Stewart, et al., *Trypanosoma cruzi* induces edematogenic responses in mice and invades cardiomyocytes and endothelial cells in vitro by activating distinct kinin receptor (B1/B2) subtypes, FASEB J. 17 (2003) 73–75.
[14] A. Geiger, C. Hirtz, T. Becue, E. Bellard, D. Centeno, D. Gargani, et al., Exocytosis and protein secretion in Trypanosoma, BMC Microbiol. 10 (2010) 20.
[15] J.M. Silverman, J. Clos, C.C. de'Oliveira, O. Shirvani, Y. Fang, C. Wang, et al., An exosome-based secretion pathway is responsible for protein export from *Leishmania* and communication with macrophages, J. Cell Sci. 123 (2010) 842–852.
[16] B.J. Backes, J.L. Harris, F. Leonetti, C.S. Craik, J.A. Ellman, Synthesis of positional-scanning libraries of fluorogenic peptide substrates to define the extended substrate specificity of plasmin and thrombin, Nat. Biotechnol. 18 (2000) 187–193.
[17] J.L. Harris, B.J. Backes, F. Leonetti, S. Mahrus, J.A. Ellman, C.S. Craik, Rapid and general profiling of protease specificity by using combinatorial fluorogenic substrate libraries, Proc. Natl. Acad. Sci. U. S. A. 97 (2000) 7754–7759.
[18] S.S. Cotrin, L. Puzer, W.A. de Souza Judice, L. Juliano, A.K. Carmona, M.A. Juliano, Positional-scanning combinatorial libraries of fluorescence resonance energy transfer peptides to define substrate specificity of carboxydipeptidases: assays with human cathepsin B, Anal. Biochem. 335 (2004) 244–252.
[19] E. Wirtz, S. Leal, C. Ochatt, G.A. Cross, A tightly regulated inducible expression system for conditional gene knock-outs and dominant-negative genetics in *Trypanosoma brucei*, Mol. Biochem. Parasitol. 99 (1999) 89–101.
[20] H. Hirumi, K. Hirumi, Continuous cultivation of *Trypanosoma brucei* blood stream forms in a medium containing a low concentration of serum protein without feeder cell layers, J. Parasitol. 75 (1989) 985–989.
[21] V. Hannaert, M.A. Albert, D.J. Rigden, M.T. da Silva Giotto, O. Thiemann, R.C. Garratt, et al., Kinetic characterization, structure modelling studies and crystallization of *Trypanosoma brucei* enolase, Eur. J. Biochem. 270 (2003) 3205–3213.
[22] P.A. Bersanetti, M.C. Andrade, D.E. Casarini, M.A. Juliano, A.T. Nchinda, E.D. Sturrock, et al., Positional-scanning combinatorial libraries of fluorescence resonance energy transfer peptides for defining substrate specificity of the angiotensin I-converting enzyme and development of selective C-domain substrates, Biochemistry 43 (2004) 15729–15736.
[23] N. Lander, M.A. Chiurillo, R. Docampo, Genome editing by CRISPR/Cas9: a game change in the genetic manipulation of protists, J. Eukaryot. Microbiol. 63 (2016) 679–690.
[24] T.C. Cheng, V. Ramakrishnan, S.I. Chan, Purification and characterization of a cobalt-activated carboxypeptidase from the hyperthermophilic archaeon *Pyrococcus furiosus*, Protein Sci. 8 (1999) 2474–2486.
[25] H.S. Lee, Y.J. Kim, S.S. Bae, J.H. Jeon, J.K. Lim, S.G. Kang, et al., Overexpression and characterization of a carboxypeptidase from the hyperthermophilic archaeon *Thermococcus* sp. NA1, Biosci. Biotechnol. Biochem. 70 (2006) 1140–1147.
[26] S.H. Lee, E. Minagawa, H. Taguchi, H. Matsuzawa, T. Ohta, S. Kaminogawa, et al., Purification and characterization of a thermostable carboxypeptidase (carboxypeptidase Taq) from *Thermus aquaticus* YT-1, Biosci. Biotechnol. Biochem. 56 (1992) 1839–1844.
[27] J.E. Mace, B.J. Wilk, D.A. Agard, Functional linkage between the active site of alpha-lytic protease and distant regions of structure: scanning alanine mutagenesis of a surface loop affects activity and substrate specificity, J. Mol. Biol. 251 (1995) 116–134.
[28] M. Okai, A. Yamamura, K. Hayakawa, S. Tsutsui, K.I. Miyazono, W.C. Lee, et al., Insight into the transition between the open and closed conformations of *Thermus thermophilus* carboxypeptidase, Biochem. Biophys. Res. Commun. 484 (2017) 787–793.
[29] B. Sharma, S.N. Jamdar, B. Ghosh, P. Yadav, A. Kumar, S. Kundu, et al., Active site gate of M32 carboxypeptidases illuminated by crystal structure and molecular dynamics simulations, Biochim. Biophys. Acta 1865 (2017) 1406–1415.